

# Magnetic Resonant Mode in Superconducting $\text{Rb}_x\text{Fe}_{2-y}\text{Se}_2$

G. Friemel, J. T. Park, Yuan Li, J.-H. Kim, B. Keimer, and D. Inosov

Soon after the discovery of arsenic-free iron-selenide superconductors  $A_x\text{Fe}_{2-y}\text{Se}_2$  ( $A = \text{K}, \text{Rb}, \text{Cs}$ ), also known as 245-compounds, their unprecedented physical properties came to light, such as the coexistence of high- $T_c$  superconductivity with strong antiferromagnetism. The pairing mechanism and the symmetry of the superconducting order parameter in this family of compounds still remain among the major open questions. In the majority of other Fe-based superconductors, it is widely accepted that the strong nesting between a holelike Fermi surface at the Brillouin zone center and an electronlike one at the Brillouin zone boundary leads to the sign-changing  $s$ -wave ( $s_{\pm}$ -wave) pairing symmetry. This scenario has been supported by different experimental methods, such as angle-resolved photoemission spectroscopy (ARPES), quasi-particle interference, and inelastic neutron scattering (INS). On the other hand, recent theoretical calculations and ARPES experiments on the 245-system revealed the absence of a holelike Fermi surface at the Brillouin zone center in the electronic structure, implying that the nesting between the hole- and electronlike Fermi sheets is no longer present. Hence, several theoretical studies proposed alternative pairing scenarios with a  $d$ -wave or another type of  $s_{\pm}$ -wave symmetry. As a hallmark of sign-changing superconducting order parameter, several authors theoretically predicted a resonant mode in the magnetic excitation spectrum below the superconducting transition, yet its precise position in momentum space has remained controversial until recently [1,2].

A major complication in treating the 245-compounds theoretically arises from the presence of a crystallographic superstructure of Fe vacancies that has been consistently reported both from x-ray and neutron diffraction experiments. This  $\sqrt{5} \times \sqrt{5}$  superstructure is closely related to the static antiferromagnetic (AFM) order persisting up to the Néel temperature,  $T_N \approx 540$  K. Although most of the existing band structure calculations have so far neglected the superstructure, several others have pointed out that it may have a strong influence on the Fermi surface. However, these pronounced reconstruction effects have not been experimentally confirmed so far. Such an uncertainty in the Fermi surface geometry and its nesting properties makes it hard to predict the exact location of itinerant spin fluctuations in reciprocal space. In our recent work [2,3], we have provided experimental insight by using INS to directly probe the elementary magnetic excitations in superconducting  $\text{Rb}_2\text{Fe}_4\text{Se}_5$  (RFS).

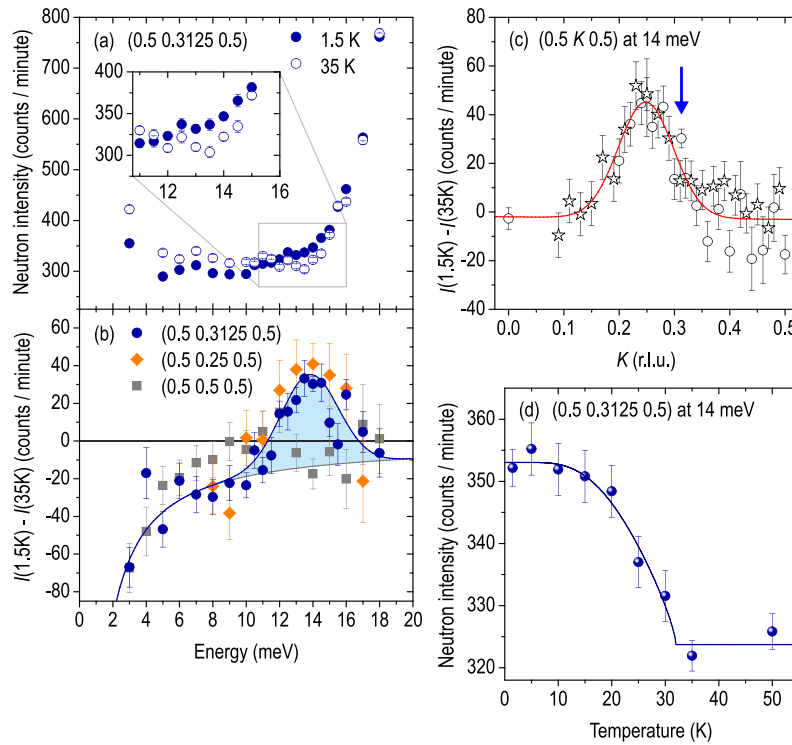


Figure 1: (a) Raw energy scans measured in the superconducting (1.5 K) and normal (35 K) states at  $\mathbf{Q} = (0.5, 0.3125, 0.5)$  and  $(0.5, 0, 0.5)$ , respectively. (b) Intensity difference between the superconducting state and the normal state at three  $\mathbf{Q}$ -vectors:  $(0.5, 0.25, 0.5)$ ,  $(0.5, 0.3125, 0.5)$ , and  $(0.5, 0.5, 0.5)$ . While there is no positive intensity at  $(0.5, 0.5, 0.5)$ , a clear resonance peak (shaded region) is observed around 14 meV both at  $(0.5, 0.25, 0.5)$  and  $(0.5, 0.3125, 0.5)$ . (c) Intensity difference of momentum scans along the Brillouin-zone boundary, measured below and above  $T_c$ . The position of the resonant mode predicted by Maier *et al.* [1] is shown by the arrow. (d) Temperature dependence of the INS intensity at 14 meV and  $\mathbf{Q} = (0.5, 0.3125, 0.5)$  that demonstrates an order-parameter-like behavior with an onset at  $T_c$ .

For this study, we have used a mosaic of RFS single crystals with a total mass of  $\sim 1$  g, grown by the Bridgman method. The nearly stoichiometric and homogeneous composition with  $\text{Rb}:\text{Fe}:\text{Se} = 0.796:1.596:2.000$  (1.99:3.99:5) has been determined by wave-length dispersive x-ray electron-probe microanalysis. The superconducting properties of the sample were characterized by magnetometry, where  $\sim 100\%$  flux exclusion was

observed in the zero-field-cooled (ZFC) measurement for temperatures up to  $T_c = 32$  K [Fig. 1(a)]. The INS experiment was performed at the thermal-neutron triple-axis spectrometer IN8 (ILL, Grenoble), with the sample mosaic mounted in the  $(HH0)/(00L)$  or  $(H00)/(00L)$  scattering planes. Here and henceforth, we are using unfolded reciprocal-space notation corresponding to the Fe sublattice, because of its simplicity and the natural correspondence to the symmetry of the observed signal.

We start with presenting the INS measurements across  $T_c$  near the  $\mathbf{Q} = (0.5 \ 0.3125 \ 0.5)$  wave vector, where the magnetic resonant mode has been theoretically predicted [1]. Figure 1 (a) displays raw energy-scan spectra recorded above and below  $T_c$  at this wave vector. In the absence of any resonant enhancement, the intensity is expected to be higher in the normal state due to the influence of the Bose factor at low energies. Already in the raw data, one can see that this is the case for all data points except a narrow energy region around 14 meV (inset). To emphasize this effect and to eliminate the energy-dependent background, we plot the temperature differences of the same datasets in Fig. 1 (b). Also shown are the difference spectra for  $\mathbf{Q} = (0.5 \ 0.5 \ 0.5)$  and  $(0.5 \ 0.25 \ 0.5)$ . A prominent peak (shaded region) is found at  $\hbar\omega_{\text{res}} \approx 14$  meV both for  $\mathbf{Q} = (0.5 \ 0.3125 \ 0.5)$  and  $\mathbf{Q} = (0.5 \ 0.25 \ 0.5)$ , which we attribute to the magnetic resonant mode. However, no such peak is observed at  $\mathbf{Q} = (0.5 \ 0.5 \ 0.5)$ . At this wave vector, the data simply follow the solid line, which is the Bose-factor difference between 1.5 K and 35 K.

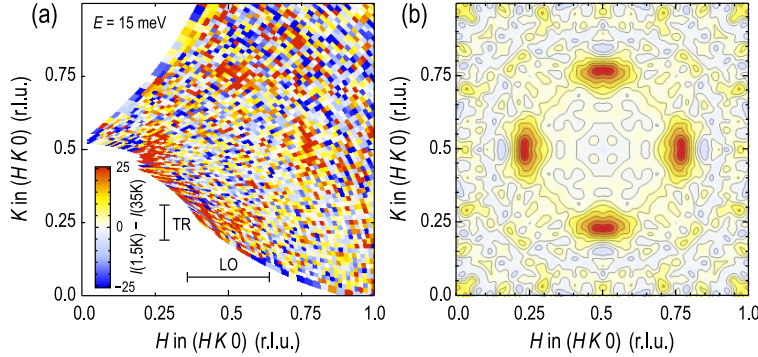


Figure 2: (a) Color map of the reciprocal space, showing intensity difference between the superconducting and normal states at  $E = 15$  meV, measured by the *FlatCone* detector. (b) The same map as in (a), rebinned on a  $81 \times 81$  grid, symmetrized with respect to the mirror planes and smoothed using a Gaussian filter with 1 pixel standard deviation.

To pin down the exact location of the resonance in  $\mathbf{Q}$ -space, we have measured momentum scans along the Brillouin-zone boundary at both temperatures. Their difference is presented in Fig. 1 (c) and suggests a maximum at the commensurate nesting wave vector  $\mathbf{Q}_{\text{res}} = (0.5 \ 0.25 \ 0.5)$ , close to the predicted resonance position,  $\mathbf{Q} = (0.5 \ 0.3125 \ 0.5)$  [1]. To verify whether the observed redistribution of spectral weight at low temperatures is related to the superconducting transition, we have also measured the temperature dependence of the resonance intensity, as shown in Fig. 1 (d). Indeed, an order-parameter-like increase of intensity below  $T_c$  is found, which is accepted as the hallmark of the magnetic resonant mode.

Furthermore, we have also mapped out the resonant enhancement of spin excitations at  $E = 15$  meV in the  $(HK0)$  scattering plane by means of the *FlatCone* multianalyzer. Figure 2 (a) shows the difference of intensity maps measured around the Brillouin-zone corner in the superconducting and normal states. In this experiment, we have observed resonant intensity at all four symmetric positions equivalent to  $(1/2 \ 1/4 \ 0)$ . In order to reduce the statistical noise in the data, we have rebinned this data set on an  $81 \times 81$  grid and symmetrized it with respect to four mirror planes of the reciprocal space, with subsequent Gaussian smoothing. The resulting intensity map is shown in Fig. 2 (b) as a contour plot. One sees that the in-plane shape of the resonant intensity takes an elliptical form, elongated transversely with respect to the vector connecting it to  $(1/2 \ 1/2 \ 0)$ . The ratio of the peak widths in the transverse and longitudinal directions results in an aspect ratio of  $\sim 2.1$  for the resonance feature.

As shown in Fig. 3 (a), this complicated pattern of resonant intensity in  $\mathbf{Q}$ -space could be successfully reproduced by a theoretical calculation of the spin susceptibility based on a  $d$ -wave symmetry of the superconducting order parameter and a tight-binding model that was introduced in Ref. 1 to describe the electronic structure of an electron-doped  $A_x\text{Fe}_2\text{Se}_2$  (for additional details, see Ref. 3). Such an agreement strongly supports the itinerant origin of the observed magnetic response, which can be traced back to the nesting of electronlike Fermi pockets, as indicated in Fig. 3 (b) by black arrows. The measured signal shows no signatures of the  $\sqrt{5} \times \sqrt{5}$  reconstruction, indicating that it originates in the metallic phase of the sample without iron-vacancy ordering, in line with the assumptions of our calculation. This distinguishes the newly observed signal from the previously reported spin-wave excitations in this class of compounds that stem from the magnetic superstructure Bragg positions in the insulating vacancy-ordered phase and are insensitive to the superconducting transition.

To conclude, we have observed the magnetic resonant mode in  $\text{Rb}_x\text{Fe}_{2-y}\text{Se}_2$  below  $T_c$ . Our finding suggests

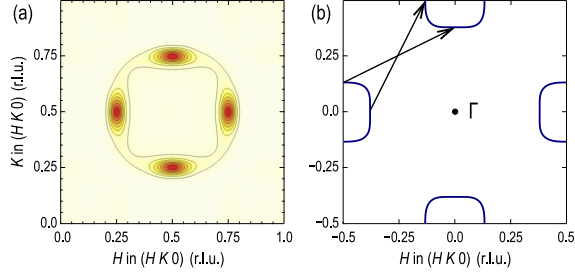


Figure 3: (a) The difference of the calculated imaginary parts of the dynamic spin susceptibility for the superconducting and normal states, taken at the resonance energy,  $\chi''_{SC}(\mathbf{Q}, \omega_{res}) - \chi''_n(\mathbf{Q}, \omega_{res})$ . An isotropic Gaussian broadening has been applied to mimic the experimental resolution. (b) The Fermi surface in the  $(H K 0)$  plane corresponds to the doping level of 0.18 electrons/Fe. The black arrows are the in-plane nesting vectors responsible for the resonance peaks revealed in our study.

unconventional pairing with a sign-changing order parameter in the 245-systems, qualitatively consistent with theoretical predictions made under the assumption of a  $d$ -wave pairing and a finite electron doping in the metallic phase volume. It evidences bulk superconductivity in our sample, consistent with the  $\sim 100\%$  flux exclusion observed in the magnetization measurements, but can also be reconciled with the microscopic segregation, or phase separation, of antiferromagnetically ordered and superconducting phases. The estimated ratios of  $\hbar\omega_{res}/k_B T_c \approx 5.1 \pm 0.4$  and  $\hbar\omega_{res}/2\Delta \approx 0.7 \pm 0.1$ , where  $\Delta$  is the superconducting energy gap, indicate moderately strong pairing, similar to other Fe-based superconductors.

#### References:

- [1] Maier, T. A., *et al.* Physical Review B **83**, 100515(R) (2011).
- [2] Park, J. T., *et al.* Physical Review Letters **107**, 177005 (2011).
- [3] Friemel, G., *et al.* arXiv:1112.1636 (2011), to be published.

#### In collaboration with:

V. Tsurkan, J. Deisenhofer, H.-A. Krug von Nidda, and A. Loidl (Augsburg University, Germany)  
A. Ivanov (Institut Laue-Langevin, Grenoble, France)  
T. A. Maier (Oak Ridge National Lab, USA)